



Published in final edited form as:

J Mol Biol. 2008 February 22; 376(3): 607–613.

Coronin-1A Stabilizes F-Actin by Bridging Adjacent Actin Protomers and Stapling Opposite Strands of the Actin Filament

Vitold E. Galkin^{1,*}, Albina Orlova¹, William Brieher², Hao Yuan Kueh², Timothy J. Mitchison², and Edward H. Egelman^{1,*}

¹Department of Biochemistry and Molecular Genetics, University of Virginia, Box 800733, Charlottesville, VA 22908-0733

²Department of Systems Biology, Harvard Medical School, Boston, MA 02115

Abstract

Coronins are F-actin binding proteins that are involved, in concert with Arp2/3, Aip1 and ADF/cofilin, in rearrangements of the actin cytoskeleton. An understanding of coronin function has been hampered by the absence of any structural data on its interaction with actin. Using electron microscopy and three-dimensional reconstruction, we show that coronin-1A binds to three protomers in F-actin simultaneously: it bridges subdomain 1 and subdomain 2 of two adjacent actin subunits along the same long-pitch strand, and it staples subdomain 1 and subdomain 4 of two actin protomers on different strands. Such a mode of binding explains how coronin can stabilize actin filaments *in vitro*. In addition, we show which residues of F-actin may participate in the interaction with coronin-1A. Human nebulin and Xin, as well as *Salmonella* invasion protein A (SipA) use a similar mechanism to stabilize actin filaments. We suggest that the stapling of subdomain 1 and subdomain 4 of two actin protomers on different strands is a common mechanism for F-actin stabilization utilized by many actin binding proteins that have no homology.

Rearrangements of the actin cytoskeleton are important for many physiological processes in the cell including cytokinesis and locomotion^{1,2}. Dozens of actin binding proteins have been shown to orchestrate actin cytoskeletal dynamics, and these include coronin, originally found in *Dicytostelium amoeba*³. The colocalization of coronin with crown-like actin structures of the cell cortex gave coronin its name. Since its discovery in amoeba, coronin has been identified in many eukaryotic organisms including yeast, nematode, fish, and mammals. Functional studies on amoeba⁴, yeast⁵, and mammalian cells⁶ suggest that coronin is directly involved in cell migration and cytokinesis.

Coronin consists of a highly conserved N-terminal extension (NE), followed by five canonical WD40 repeats, a C-terminal conserved extension (CE), followed by a unique region (U), and ends with a C-terminal coiled-coil (CC) domain. A recent crystal structure of coronin-1 shows that a portion of these highly conserved N- and C-terminal extensions form the first and the last blades of a seven-bladed β -propeller⁷. The CC-domain is involved in the oligomerization of coronin and is responsible for the bundling of actin filaments⁸. Mammals have at least six known coronin genes, and these are divided into three subclasses⁹. Type I coronins include coronin-1A, -1B, and -1C. They differ in the U-region and are expressed in most tissues, except

*To whom correspondence should be addressed: egelman@virginia.edu; phone 434-924-8210; fax 434-924-5069; galkin@virginia.edu; phone 434-243-6115; fax 434-924-5069

Publisher's Disclaimer: This is a PDF file of an unedited manuscript that has been accepted for publication. As a service to our customers we are providing this early version of the manuscript. The manuscript will undergo copyediting, typesetting, and review of the resulting proof before it is published in its final citable form. Please note that during the production process errors may be discovered which could affect the content, and all legal disclaimers that apply to the journal pertain.

coronin-1A which is found predominantly in hematopoietic cells. Type II coronins (2A and 2B) differ from Type I particularly in the CE-region, while Type III coronin (coronin-7), found only in mammals, is composed of tandem coronin repeats, but lacks the CC-region.

Coronin participates, in concert with Arp2/3, cofilin, and Aip1, in the reorganization of actin structures at the leading edge of the cell. It was shown that coronin directly binds to Arp2/3¹⁰, and inhibits F-actin nucleation by freezing the Arp2/3 complex in its inactive “open” conformation¹¹. *In vitro* experiments showed that coronin stabilizes actin filaments in dilution experiments, as well as prevents cofilin-induced F-actin depolymerization^{12,13}.

Since coronin was identified as an actin binding protein, a significant effort has been invested in establishing its actin binding region. Ironically, the actin-binding regions have been mapped to almost all parts of the protein. Originally, it was suggested¹⁴ that all regions except the N-terminus and the β -propeller domain interact with F-actin. Subsequently, it was shown¹⁵ that the N-terminal 1-34 residues along with residues 111-204 of a β -propeller region were important for F-actin binding. Another work proposed the linker region as an actin binding site, while binding to the cell membrane was the only role suggested for the β -propeller region¹⁶. Finally, residues 297-461 that contain a part of the β -propeller domain in addition to the CE-domain, U-domain, and CC-domain were shown to be involved in binding to actin filaments¹⁷. All of these studies were based on truncated mutants that contained fragments of the full length coronin. Alanine scanning mutagenesis of the full length protein revealed that mutation of Arg30 completely abolished interaction of coronin-1B with F-actin¹³. The residues of actin involved in the interaction with coronin remain unknown, as well as the position of coronin on the actin filament.

We used electron microscopy and image analysis to evaluate how coronin-1A binds to actin filaments. Samples were prepared for EM by incubating 1.5 μ M actin with 4-5 μ M coronin. We formed coronin-actin complexes by both polymerizing actin in the presence of coronin and by adding coronin to pre-formed actin filaments, and found no significant differences in the binding. Coronin can form oligomers^{18,14} which ultimately results in coronin-dependent bundling of F-actin^{5,13}. Since incubations of longer than an hour led to bundle formation (data not shown), and bundles are more difficult objects for image analysis, we used short incubation times to limit the extent of coronin-induced bundling. Images of negatively-stained, pure F-actin were consistent with a 9-10nm diameter fiber (Fig 1a). In contrast, actin filaments incubated with coronin-1A for 40 min were more massive reflecting extensive decoration with coronin (Fig. 1b). Attempts to use electron cryo-microscopy of unstained frozen-hydrated samples were unsuccessful, due to the fact that the coronin fell off the actin filaments at some stage during specimen preparation. A similar loss of fimbrin decoration of F-actin during preparation for electron cryo-microscopy has been described¹⁹.

We generated a global, three-dimensional reconstruction of coronin decorated filaments such as those shown in Fig. 1b to locate the position of coronin on the actin filament. The overall three-dimensional reconstruction (Fig. 2b) has a pronounced additional mass due to the coronin-1A when compared with a control pure F-actin reconstruction (Fig. 2a). This contiguous mass makes major contacts with three different actin protomers. Therefore, a single actin protomer makes contacts with three different coronin molecules. Mapping the contacts from these three different coronin molecules onto a single actin, the interface involves: SD2 (Fig. 2b, red asterisk), SD1 (Fig. 2b, blue asterisk), and SD4 (Fig. 2b, green asterisk).

The global reconstruction (Fig. 2b) suggests that the coronin density reflects a single mode of binding of coronin to F-actin, where coronin simultaneously interacts with these three protomers on F-actin. An alternative possibility is that the binding to these three sites is independent, and the density that we observe in the overall reconstruction may be an average

of several different modes of binding. To distinguish between these two possibilities we used a model-based cross-correlation sorting (Fig. 2c). One of the great advantages of the Iterative Helical Real Space Reconstruction (IHRSR) approach to helical reconstruction is that we can readily sort segments into separate classes without assuming that all filaments are homogeneous polymers²⁰. Using this approach, almost 50% of segments yielded the best correlation with the naked F-actin model, and thus were classified as poorly occupied. The reconstruction of this class (not shown) was not, in fact, that of naked F-actin, but revealed traces of coronin at the position similar to that observed in the overall reconstruction. Approximately 50% of the decorated segments had the highest correlation with the model where coronin interacts simultaneously with all three sites (Fig. 2d), while segments assigned to the “SD4” class (where coronin is only binding to SD4 of one each actin protomer) failed to converge to a stable reconstruction using the IHRSR method (data not shown). This suggests that the segments assigned to this “SD4” class were heterogeneous and probably contained coronin bound in an irregular manner to actin. Approximately 30% of decorated segments showed coronin bound to the interface between SD1 and SD2, but lacking the contact with SD4 (Fig 2d-e, red arrows). The additional density due to coronin-1A in these two reconstructions after sorting (Fig. 2d,e) is noticeably larger than that in the overall reconstruction (Fig. 2b), showing that the removal of poorly occupied segments significantly improves the reconstruction of the complex. We estimate the resolution of the improved reconstruction to be ~ 21 Å using the Fourier Shell Correlation (FSC) 0.5 criterion. As we will show, the mass due to coronin in the improved reconstructions is more consistent with what is known about the size and shape of coronin than is the mass in the global reconstruction.

To build a quasi-atomic model of the coronin-1A-F-actin complex we used a recent crystal structure of murine coronin-1⁷. The coronin crystal structure lacks the first 7 N-terminal residues, the U-region, and the CC-domain (65 of 461 residues). When we threshold our map to account for the full molecular volume due to actin, the density due to coronin accommodates the crystal structure. Considering that the crystal structure itself is lacking $\sim 15\%$ of coronin-1A residues (namely the U- and CC-domains), we assume that the U- and CC-domains are disordered when coronin is bound to F-actin, and thus not visible in our reconstruction. An argument in support of this possibility is that the coiled-coil domain, which is involved in oligomerization⁸ is likely to be flexible. We therefore think that this reconstruction after sorting is consistent with F-actin being fully occupied by coronin.

The observed oligomerization of coronin in solution raises a question as to whether the coronin density that we observe might be due to bound dimers or higher oligomers. It is possible that the dimers dissociate upon binding to F-actin. Alternatively, two scenarios can be imagined where the species bound to F-actin is dimeric: firstly, one coronin molecule is attached to F-actin, while the second one in a dimer is disordered; secondly, two adjacent coronins attached to F-actin form a dimer via flexible CC-domains. We think that the diameters of the F-actin filaments decorated with coronin-1A (~ 170 Å) argues against the disordered dimer possibility, because even if the second coronin is not visible in the reconstruction due to disorder, it should contribute to the filament width in the EM pictures. In terms of the second scenario, we cannot exclude the possibility that dimers of coronin bind to F-actin, just as dimers (HMM) of the myosin S1 actin-binding domain can decorate F-actin²¹.

We took advantage of mutagenesis experiments that helped map the actin binding site on coronin to orient the crystal structure of coronin-1 into our map of coronin-decorated F-actin. It has been shown¹³ that alanine substitution of Arg30 (R30A) attenuated the ability of coronin to induce cables in S2 cells, while the charge-reversal mutation (R30D) completely abolished cable formation. In addition, the R30D mutant did not bind F-actin *in vitro*. We found that it was not possible to fit the coronin-1A crystal structure into our map with R30 not in proximity to F-actin. Due to the shape-based constraints, the only reasonable orientation of the coronin

atomic model was when R30 of coronin (Fig. 3b, red spheres) was placed facing residues 78-82 of SD1 of actin (Fig. 3b, magenta ribbons). In addition to these residues, coronin is making a contact with residues 120-125 of actin, which form a loop on the rear surface of actin's SD1 (Fig. 3b, magenta ribbons), and the C-terminal residues 362-368 also located in SD1 of actin (Fig. 3b, magenta ribbons). SD2 of actin is involved in the interaction with coronin via residues 39-42, and 49-52 located in the DNase I-binding loop (Fig. 3b, magenta ribbons). Coronin-1A also makes a contact with a protomer on the opposite strand. We observe an extensive contact of coronin with the 221-238 protrusion in SD4 of F-actin (Fig. 3b, orange ribbons). Interestingly, this region is one of the insertions in actin absent in the actin prokaryotic homologs MreB²² and ParM^{23,24}, and was shown to interact with nebulin²⁵, Xin²⁶, *Salmonella* invasion protein A (SipA)²⁷, and Arg-kinase²⁸. Also there is a weaker contact with residues 322-325 in SD3 of the adjacent protomer along the same long-pitch strand (Fig. 3b, orange ribbons).

How can these results be reconciled with the mutagenesis data showing that only one residue, Arg30, is crucial for coronin binding to F-actin? Even if coronin has what appears at low resolution to be an extensive interface with SD2 and SD1 of F-actin, it is possible that the interaction of Arg30 with the back side of SD1 is a key determinant of this interface. It is also possible that the primary interaction of Arg30 with F-actin activates other coronin residues to form multiple bonds with the actin filament. At the current resolution of ~21 Å we cannot see what conformational changes might be taking place within coronin when bound to F-actin, nor see this interface at an atomic level of detail. Our sorting by modes of binding (Fig. 2) shows that coronin cannot bind to SD4 without being attached to the SD1/2 interface on F-actin. However, it can bind to SD1/2 without binding to SD4. This strongly suggests that to staple together the two strands of F-actin, coronin binds first to the SD1/2 interface, and this interaction allows coronin binding to an additional site located on SD4 of an actin protomer within the opposite long-pitch helical strand.

We analyzed which residues of coronin may be involved in the interaction with SD4 of F-actin, and these are residues 20-23 (Fig. 3c, red spheres), residues 65-67 (Fig. 3c, green spheres), residues 329-331 (Fig. 3c, magenta spheres), and residues 353-358 (Fig. 3c, cyan spheres). Interestingly, these residues span the entire coronin amino acid sequence. The seemingly conflicting results on coronin residues involved in interactions with actin obtained using truncated mutants may reflect the non-contiguous regions in coronin's primary sequence that are involved in the interaction with SD4. It may not be a coincidence that our identification of residues 20-23 is consistent with one set of results¹⁵, while our identification of residues 323-331 and 353-358 agrees with other observations^{14,17}.

One of the most important coronin partners in the cell is the Arp2/3 complex, and Arp2/3 was shown to bind to the coiled-coil domain of coronin¹⁰. Phosphorylation of Ser2 on coronin by PKC abolishes this interaction²⁹. Importantly, F-actin binding increases the apparent affinity of the coronin-Arp2/3 interaction *in vivo*²⁹. The coiled-coil domain is missing in the crystal structure, and to determine a possible location for the missing C-terminal 59 residues we represented the last residue in the crystal structure (Arg402) with cyan spheres (Fig. 3b). The orientation of coronin in our quasi-atomic model brings Arg402 to the outer surface of the complex, suggesting that the CC-domain would be facing away from the actin filament. This orientation of the CC-domain is consistent with increased interaction of Arp2/3 with coronin in the presence of F-actin²⁹. Since Ser2 is also missing in the crystal structure due to disorder, we represented the first N-terminal residue present in the crystal (Ser8) with green spheres (Fig. 3b). The location of the N-terminus at the outer surface of the coronin-F-actin complex suggests that the short flexible N-terminal region containing Ser2 is fully accessible to PKC even when coronin is attached to F-actin. We may speculate that coronin is always attached to

F-actin, and works as a trap for Arp2/3: it keeps Arp2/3 inactive, but close to its target - F-actin.

Coronin 1b stabilizes vertebrate actin filaments *in vitro* from dilution-induced depolymerization¹³ while yeast coronin does not save yeast F-actin from depolymerization⁵. Our model suggests that coronin-1A, like coronin-1B, should stabilize F-actin - it not only connects two adjacent actin protomers within one strand, but also staples together protomers on two different strands. To test if coronin-1A stabilizes actin filaments, we compared the rate of depolymerization of single, coronin decorated filaments to undecorated filaments using fluorescence microscopy (Fig. 4). Fluorescently labeled actin was polymerized in the absence or presence of coronin-1A in a perfusion chamber that was previously coated with the actin crosslinking protein filamin to immobilize the actin filaments on the glass. After polymerizing for 90 seconds, the contents of the chamber were replaced with 3 chamber volumes of latrunculin in buffer and a timelapse sequence was recorded to obtain the actin off rate. Actin alone depolymerized at a rate of 1.8 subunits sec⁻¹ while actin filaments co-assembled with coronin-1A disassembled at 0.43 subunits sec⁻¹ (Fig. 4). Therefore, coronin-1A stabilizes F-actin against dilution-induced depolymerization in a defined system consistent with our interpretation of coronin 1A's interaction with the actin filament.

We have observed such a stapling mode of binding for three other actin binding proteins that stabilize F-actin or actin bundles—the muscle proteins nebulin²⁵ and Xin²⁶, and *Salmonella* protein SipA²⁷. Nebulin is a giant muscle protein (600-900 kDa) that contains ~200 copies of a 35-residue module, each believed to contain an actin-binding site³⁰, while SipA, is an actin-binding protein that promotes efficient bacterial entry into host cells³¹. There is no detectable sequence homology among coronin, SipA, Xin and nebulin. The common mode of interaction may therefore represent convergent evolution, where all of these proteins employ different detailed interactions with actin to modulate an intrinsic instability in the actin polymer.

Acknowledgments

This work was supported by NIH grants GM081303 (E.H.E.) and GM023928 (T.J.M.).

Reference List

1. Satterwhite LL, Pollard TD. Cytokinesis. *Curr. Opin. Cell Biol* 1992;4:43–52. [PubMed: 1313686]
2. Pollard TD, Borisy GG. Cellular motility driven by assembly and disassembly of actin filaments. *Cell* 2003;112:453–465. [PubMed: 12600310]
3. de Hostos EL, Bradtke B, Lottspeich F, Guggenheim R, Gerisch G. Coronin, an actin binding protein of *Dictyostelium discoideum* localized to cell surface projections, has sequence similarities to G protein beta subunits. *EMBO J* 1991;10:4097–4104. [PubMed: 1661669]
4. De Hostos EL, et al. *Dictyostelium* mutants lacking the cytoskeletal protein coronin are defective in cytokinesis and cell motility. *J. Cell Biol* 1993;120:163–173. [PubMed: 8380174]
5. Goode BL, et al. Coronin promotes the rapid assembly and cross-linking of actin filaments and may link the actin and microtubule cytoskeletons in yeast. *J. Cell Biol* 1999;144:83–98. [PubMed: 9885246]
6. Cai L, Marshall TW, Uetrecht AC, Schafer DA, Bear JE. Coronin 1B coordinates Arp2/3 complex and cofilin activities at the leading edge. *Cell* 2007;128:915–929. [PubMed: 17350576]
7. Appleton BA, Wu P, Wiesmann C. The crystal structure of murine coronin-1: a regulator of actin cytoskeletal dynamics in lymphocytes. *Structure* 2006;14:87–96. [PubMed: 16407068]
8. Oku T, et al. Homotypic dimerization of the actin-binding protein p57/coronin-1 mediated by a leucine zipper motif in the C-terminal region. *Biochem. J* 2005;387:325–331. [PubMed: 15601263]
9. Uetrecht AC, Bear JE. Coronins: the return of the crown. *Trends Cell Biol* 2006;16:421–426. [PubMed: 16806932]
10. Humphries CL, et al. Direct regulation of Arp2/3 complex activity and function by the actin binding protein coronin. *J. Cell Biol* 2002;159:993–1004. [PubMed: 12499356]

11. Rodal AA, et al. Conformational changes in the Arp2/3 complex leading to actin nucleation. *Nat. Struct. Mol. Biol* 2005;12:26–31. [PubMed: 15592479]
12. Brieher WM, Kueh HY, Ballif BA, Mitchison TJ. Rapid actin monomer-insensitive depolymerization of *Listeria* actin comet tails by cofilin, coronin, and Aip1. *J. Cell Biol* 2006;175:315–324. [PubMed: 17060499]
13. Cai L, Makhov AM, Bear JE. F-actin binding is essential for coronin 1B function in vivo. *J. Cell Sci* 2007;120:1779–1790. [PubMed: 17456547]
14. Spoerl Z, Stumpf M, Noegel AA, Hasse A. Oligomerization, F-actin interaction, and membrane association of the ubiquitous mammalian coronin 3 are mediated by its carboxyl terminus. *J. Biol. Chem* 2002;277:48858–48867. [PubMed: 12377779]
15. Oku T, et al. Two regions responsible for the actin binding of p57, a mammalian coronin family actin-binding protein. *Biol. Pharm. Bull* 2003;26:409–416. [PubMed: 12673016]
16. Gatfield J, Albrecht I, Zanolari B, Steinmetz MO, Pieters J. Association of the leukocyte plasma membrane with the actin cytoskeleton through coiled coil-mediated trimeric coronin 1 molecules. *Mol. Biol. Cell* 2005;16:2786–2798. [PubMed: 15800061]
17. Liu CZ, Chen Y, Sui SF. The identification of a new actin-binding region in p57. *Cell Res* 2006;16:106–112. [PubMed: 16467882]
18. Asano S, Mishima M, Nishida E. Coronin forms a stable dimer through its C-terminal coiled coil region: an implicated role in its localization to cell periphery. *Genes Cells* 2001;6:225–235. [PubMed: 11260266]
19. Hanein D, Matsudaira P, DeRosier DJ. Evidence for a conformational change in actin induced by fimbrin (N375) binding. *J. Cell Biol* 1997;139:387–396. [PubMed: 9334343]
20. Egelman EH. The iterative helical real space reconstruction method: surmounting the problems posed by real polymers. *J. Struct. Biol* 2007;157:83–94. [PubMed: 16919474]
21. Katayama E. Quick-freeze deep-etch electron microscopy of the actin-heavy meromyosin complex during the in vitro motility assay. *J. Mol. Biol* 1998;278:349–367. [PubMed: 9571057]
22. Galkin VE, VanLoock MS, Orlova A, Egelman EH. A new internal mode in F-actin helps explain the remarkable evolutionary conservation of actin's sequence and structure. *Cur. Biol* 2002;12:570–575.
23. van den Ent F, Moller-Jensen J, Amos LA, Gerdes K, Lowe J. F-actin-like filaments formed by plasmid segregation protein ParM. *EMBO J* 2002;21:6935–6943. [PubMed: 12486014]
24. Orlova A, et al. The structure of bacterial ParM filaments. *Nat. Struct. Mol. Biol* 2007;14:921–926. [PubMed: 17873883]
25. Lukoyanova N, et al. Each actin subunit has three nebulin-binding sites: Implications for steric blocking. *Cur. Biol* 2002;12:383–388.
26. Cherepanova O, et al. Xin-repeats and nebulin-like repeats bind to F-actin in a similar manner. *J. Mol. Biol* 2006;356:714–723. [PubMed: 16384582]
27. Galkin VE, et al. The bacterial protein SipA polymerizes G-actin and mimics muscle nebulin. *Nat. Struct. Biol* 2002;9:518–521. [PubMed: 12055622]
28. Galkin VE, Orlova A, Koleske AJ, Egelman EH. The Arg non-receptor tyrosine kinase modifies F-actin structure. *J. Mol. Biol* 2005;346:565–575. [PubMed: 15670605]
29. Cai L, Holowecyj N, Schaller MD, Bear JE. Phosphorylation of coronin 1B by protein kinase C regulates interaction with Arp2/3 and cell motility. *J. Biol. Chem* 2005;280:31913–31923. [PubMed: 16027158]
30. Wang K, et al. Human skeletal muscle nebulin sequence encodes a blueprint for thin filament architecture. Sequence motifs and affinity profiles of tandem repeats and terminal SH3. *J. Biol. Chem* 1996;271:4304–4314. [PubMed: 8626778]
31. Galan JE. Salmonella interactions with host cells: type III secretion at work. *Annu. Rev. Cell Dev. Biol* 2001;17:53–86. [PubMed: 11687484]
32. Egelman EH. A robust algorithm for the reconstruction of helical filaments using single-particle methods. *Ultramicroscopy* 2000;85:225–234. [PubMed: 11125866]
33. Frank J, et al. SPIDER and WEB: Processing and visualization of images in 3D electron microscopy and related fields. *J. Struct. Biol* 1996;116:190–199. [PubMed: 8742743]

34. Galkin VE, Orlova A, Lukoyanova N, Wriggers W, Egelman EH. Actin Depolymerizing Factor Stabilizes an Existing State of F-Actin and Can Change the Tilt of F-Actin Subunits. *J. Cell Biol* 2001;153:75–86. [PubMed: 11285275]
35. Pettersen EF, et al. UCSF Chimera--a visualization system for exploratory research and analysis. *J. Comput. Chem* 2004;25:1605–1612. [PubMed: 15264254]
36. Schutt CE, Myslik JC, Rozycki MD, Goonesekere NCW, Lindberg U. The structure of crystalline profilin: β -actin. *Nature* 1993;365:810–816. [PubMed: 8413665]

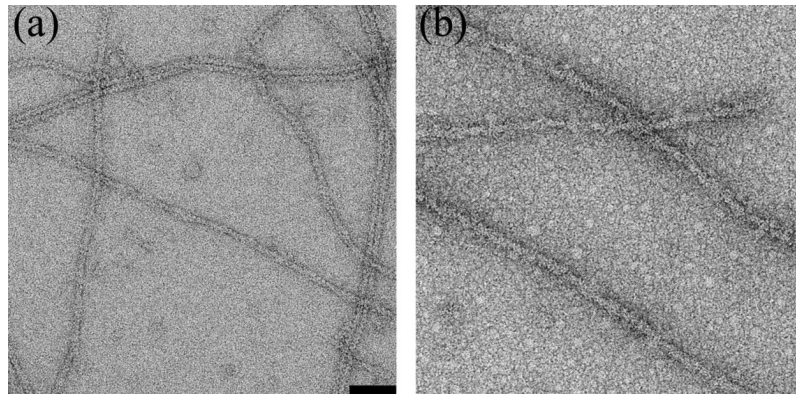


Fig. 1.

Electron micrographs of negatively stained pure F-actin (a), and F-actin after incubation with coronin-1A (b). The space bar is 500 Å. G-actin (10 μM) was polymerized in 10mM Tris-HCl buffer (pH 7.7), 0.1 mM ATP, 40 mM KCl, 2mM MgCl₂ for ~ 2 hr. Then F-actin (1.5 μM) was incubated with coronin 1A (4-5 μM) for 4-10 min before application to carbon coated glow discharged EM grids. The grids were stained with 1% uranyl acetate (w/v) and imaged in a Tecnai 12 electron microscope (80 keV, × 30,000 magnification). Images were recorded on film, and negatives were scanned with a Nikon Coolscan 8000 densitometer at a raster of 4.2 Å/pixel.

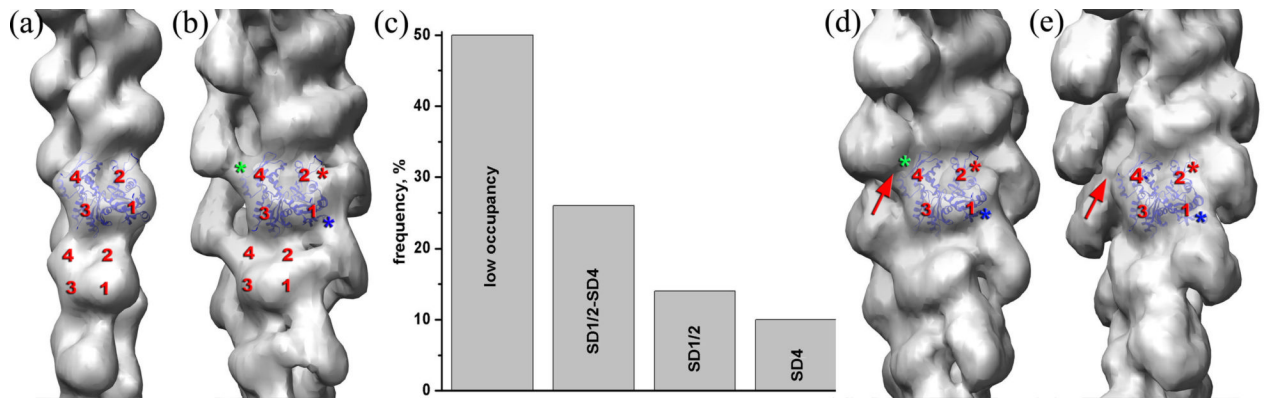


Fig. 2. The IHRSR method³², along with the SPIDER package³³, were used to generate an overall reconstruction from 10,954 overlapping segments (each 416 Å long) of actin filaments decorated with coronin-1A (b). For comparison, a three-dimensional reconstruction of pure F-actin³⁴ is shown (a). The overall reconstruction of actin decorated with coronin (b) reveals a substantial additional mass which connects SD1 and SD2 of two adjacent actin protomers within the same long pitch helical strand, while also bridging the two strands via the interaction with SD4 of an actin protomer on the opposite strand. Three different coronin-1A molecules interact with three subdomains (SD) of every actin protomer: SD2 (b, red asterisk), SD1 (b, blue asterisk), and SD4 (b, green asterisk). Three model volumes were created with additional density attached to each of these three sites simultaneously (SD1/SD2, SD4), to only the SD1/SD2 interface, and finally only to SD4 of actin. A fourth reference volume was created using naked F-actin, and the four reference volumes were projected and cross-correlated with the 10,954 image segments. The frequency distribution found for these four classes is shown in (c). Each class was reconstructed separately, starting from a featureless solid cylinder. The “SD1/2-SD4” class (n=2,850) converged to a twist of 165.5° per subunit with an axial rise per subunit of 27.4 Å, the “SD1/2” class (n=1,528) reached a stable solution of 165.5°/26.7Å, while “SD4” class (n=1002) failed to converge to any meaningful volume. Segments having the best correlation with the naked F-actin (n=5,574) converged to a 165.5°/27.4 Å symmetry. The reconstructions of the “SD1/2-SD4” (d) and “SD1/2” (e) classes are similar, except that in the “SD1/2” class the contact between coronin-1B and SD4 is missing (d and e, red arrow).

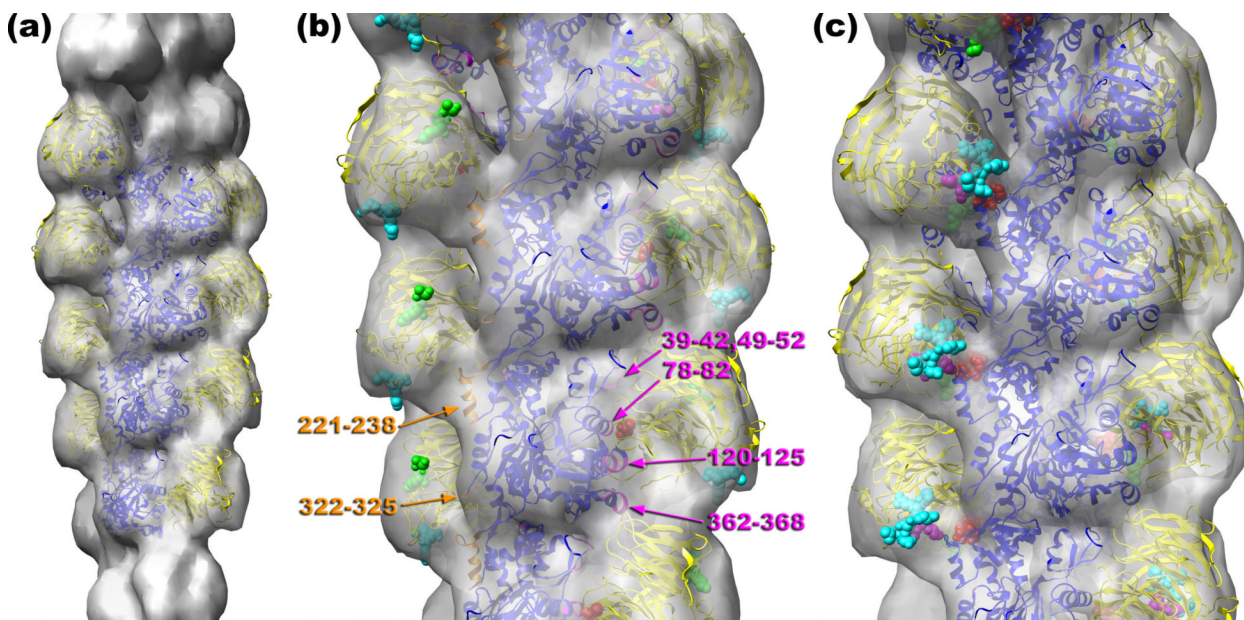
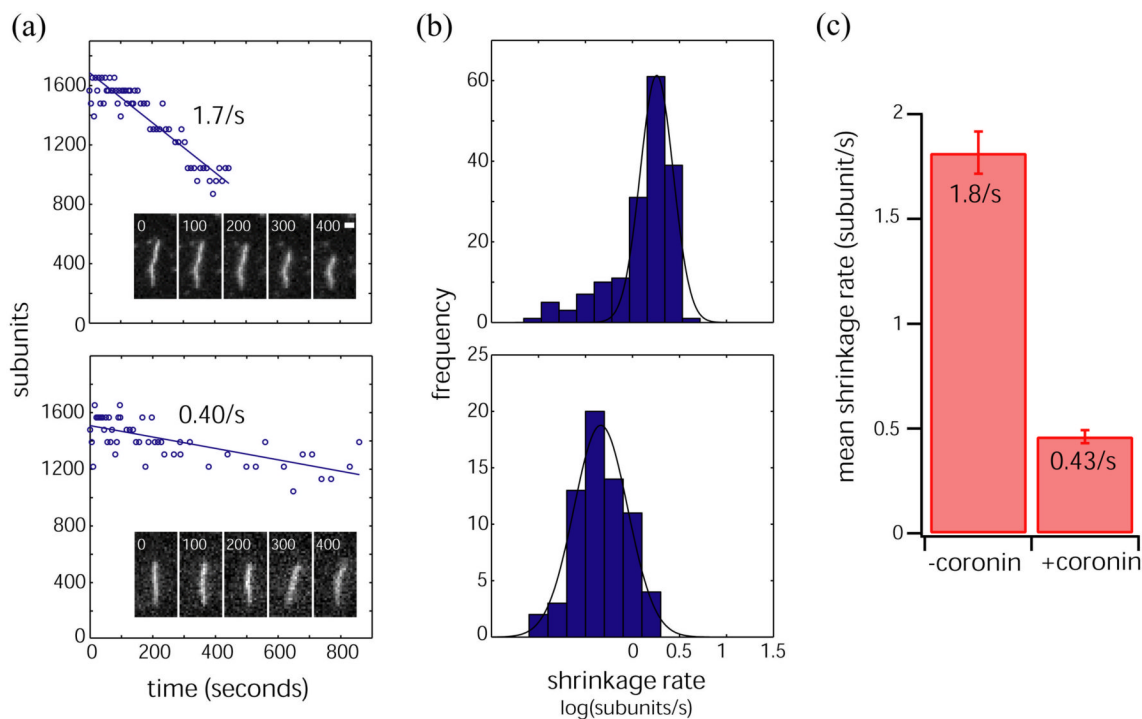


Fig. 3.

To reduce heterogeneity and improve the appearance of coronin the “SD1/2-SD4” class was sorted by the actin twist into three groups: 162° , 166° , and 168° . The reconstruction of the 168° class ($n=963$) possessed the largest coronin density, and it was used for modeling. The Chimera software³⁵ was used to build up an atomic model of the coronin 1A-F-actin complex (a), which has actin protomers in blue and coronin in yellow. Crystal structures of G-actin³⁶ and murine coronin-1⁷ were docked into the reconstruction manually. The detailed view of the atomic model is shown in (b). Arg30 of coronin-1B is represented as red spheres, with the N-terminus and C-terminus shown as green and cyan spheres, respectively. Actin residues that are at the interface between coronin-1A and F-actin are marked: residues 78-82, 120-125, and 362-368 of SD1, 39-42, and 49-52 of SD2 (magenta ribbons), residues 221-238 of SD4, and finally residues 322-325 of SD3 (orange ribbons). The second site of binding of coronin to SD4 of F-actin (c) involves residues 20-23 (red spheres), residues 65-67 (green spheres), residues 329-331 (magenta spheres), and residues 353-358 (cyan spheres). The coordinates of the model are available at <http://people.virginia.edu:80/~ehe2n/coronin.html>

**Fig. 4.**

Coronin stabilizes the actin filament. Actin ($6 \mu\text{M}$, with $\sim 30\%$ labeled on lysines with Alexa-647-NHS ester) was polymerized in a perfusion chamber coated with $10 \mu\text{g/ml}$ filamin and subsequently depolymerized by washout of unpolymerized monomer. Depolymerization of single actin filaments was imaged using widefield fluorescence microscopy. Reactions were carried out either in the absence or in the presence of $6 \mu\text{M}$ coronin. a) Representative single filaments depolymerizing in the absence (top) or presence (bottom) of coronin. Shown are successive timelapse images of filaments (time elapsed shown on top, scale bar = 1 micron), along with corresponding graphs showing total filament length as a function of time. Shrinkage rates are obtained from best straight line fits to the data. b) Histogram of shrinkage rates in the absence (top) or presence (bottom) of coronin. Histograms are fit to a single Gaussian to obtain the mean shrinkage rate. c) Bar chart showing the mean shrinkage rate in the absence (left) or presence (bottom) of coronin. Error bars represent 95% confidence bounds. Coronin reduced the mean shrinkage rate from 1.8/s to 0.43/s.